ChemPubSoc Europe

DOI: 10.1002/chem.201802886

CHEMISTRY A European Journal Communication

C–H Bond Activation

Accelerated Ru–Cu Trinuclear Cooperative C–H Bond Functionalization of Carbazoles: A Kinetic and Computational Investigation

Alexander W. Jones,[a] Christian K. Rank,[a] Yanik Becker,[a] Christian Malchau,[a] Ignacio Funes-Ardoiz,[b] Feliu Maseras,*[b, c] and Frederic W. Patureau*[a]

Abstract: The mechanism of a trinuclear cooperative dehydrogenative C–N bond-forming reaction is investigated in this work, which avoids the use of chelate-assisting directing groups. Two new highly efficient Ru/Cu co-catalyzed systems were identified, allowing orders of magnitude greater TOFs than the previous state of the art. In-depth kinetic studies were performed in combination with advanced DFT calculations, which reveal a decisive rate-determining trinuclear Ru–Cu cooperative reductive elimination step (CRE).

Most textbooks teach organometallic catalysis as simple mononuclear catalytic cycles, with well-behaved oxidative additions, transmetalations, and reductive elimination steps. This simplified view is very practical to help understand catalysis. In contrast, optimizing, characterizing, and utilizing polynuclear cooperative effects in catalysis is complicated, time-consuming, and costly. This is why very few research groups have been able to integrate cooperative polynuclearity in their mechanisms.[1]

In this context, the development of efficient and selective methods for the construction of C–C and C–heteroatom bonds is of primordial importance.[2] C–N bonds are notably prevalent in the scaffold of countless biologically and pharmaceutically relevant compounds. Unfortunately, most established approaches for the catalytic construction of C–N bonds[3] require pre-synthesized starting materials, thus lengthening synthetic routes and their atom- and step-economy footprints. In contrast, the direct transformation of a C–H bond into a C–N bond, particularly in a dehydrogenative fashion, is a more straightforward strategy.[4] Most known C–H bond activation methods, however, require the coordinative assistance of a directing group (DG) in order to achieve regioselective transformations. Moreover, these DGs are rarely desired in the targeted molecular scaffolds. Therefore, the synthetic utility of those methods is typically undermined by the, often laborious, DG removal. Clearly, the development of synthetic methods that avoid the coordinative assistance of a DG constitute a research priority, wherein the catalyst is designed to control both C–H bond activation reactivity and selectivity. In this study, we will attempt to demonstrate the suitability of a cooperative polynuclear catalytic approach for DG-free C–H bond functionalization in a seemingly simple test reaction (Scheme 1).

In an early 2013 communication, some of us delivered preliminary results about a Ru/Cu co-catalyzed dehydrogenative homo-coupling of two carbazoles to form a unique C1–N bicarbazole product (Scheme 1).[4a,5] This early method, however, suffered from very low turn-over-frequencies (TOFs), thereby requiring up to two weeks of reaction time. We therefore decided to re-optimize this reaction, notably by ligand/catalyst screening (**Ru-complex1** to **Ru-complex11**, and ligand $\mathbf{L^1}$ to $\mathbf{L^8}$, see Supporting Information). This allowed the identification of two new extremely active ruthenium pre-catalysts: **[(Ru-complex6)$_2$]** (phosphine-free), and **[(Ru-complex3)$_2$L^4]** (ligand $\mathbf{L^4}$: 1,1′-bis(diphenylphosphino)ferrocene (dppf), Scheme 1), the latter affording C1–N bicarbazole product **2a** in significantly improved 80% yield. Interestingly, and in contrast to the dppf ligand, the well-known[3] XPhos ligand ($\mathbf{L^2}$) did not perform well (**2a**, 40%), although it had been successfully utilized in a previous Ru catalyzed C–H functionalization reaction by Ackermann.[6] Other iron-based additives than the dppf ligand $\mathbf{L^4}$ were also tested, including ordinary ferrocene (**2a**, 69%), or alternatively $Fe(OAc)_2$ (**2a**, 69%); however, none were found as efficient (**2a**, 80%). The main objective of the following study is to investigate the kinetic profiles of those complex polymetallic systems and to propose a general mechanistic model.

The two new best catalytic systems based on **[(Ru-complex6)$_2$]** and **[(Ru-complex3)$_2$L^4]** were then evaluated in the

[a] A. W. Jones, C. K. Rank, Y. Becker, C. Malchau, Prof. Dr. F. W. Patureau
FB Chemie, TU Kaiserslautern
Erwin Schrödinger Strasse 52, 67663 Kaiserslautern (Germany)
E-mail: patureau@chemie.uni-kl.de

[b] Dr. I. Funes-Ardoiz, Prof. Dr. F. Maseras
Institute of Chemical Research of Catalonia (ICIQ)
The Barcelona Institute of Science and Technology
Avgda. Països Catalans, 16, 43007 Tarragona (Spain)
E-mail: fmaseras@ICIQ.ES

[c] Prof. Dr. F. Maseras
Departament de Química
Universitat Autònoma de Barcelona
08193 Bellaterra (Spain)

Supporting information and the ORCID identification number(s) for the author(s) of this article can be found under: https://doi.org/10.1002/chem.201802886.

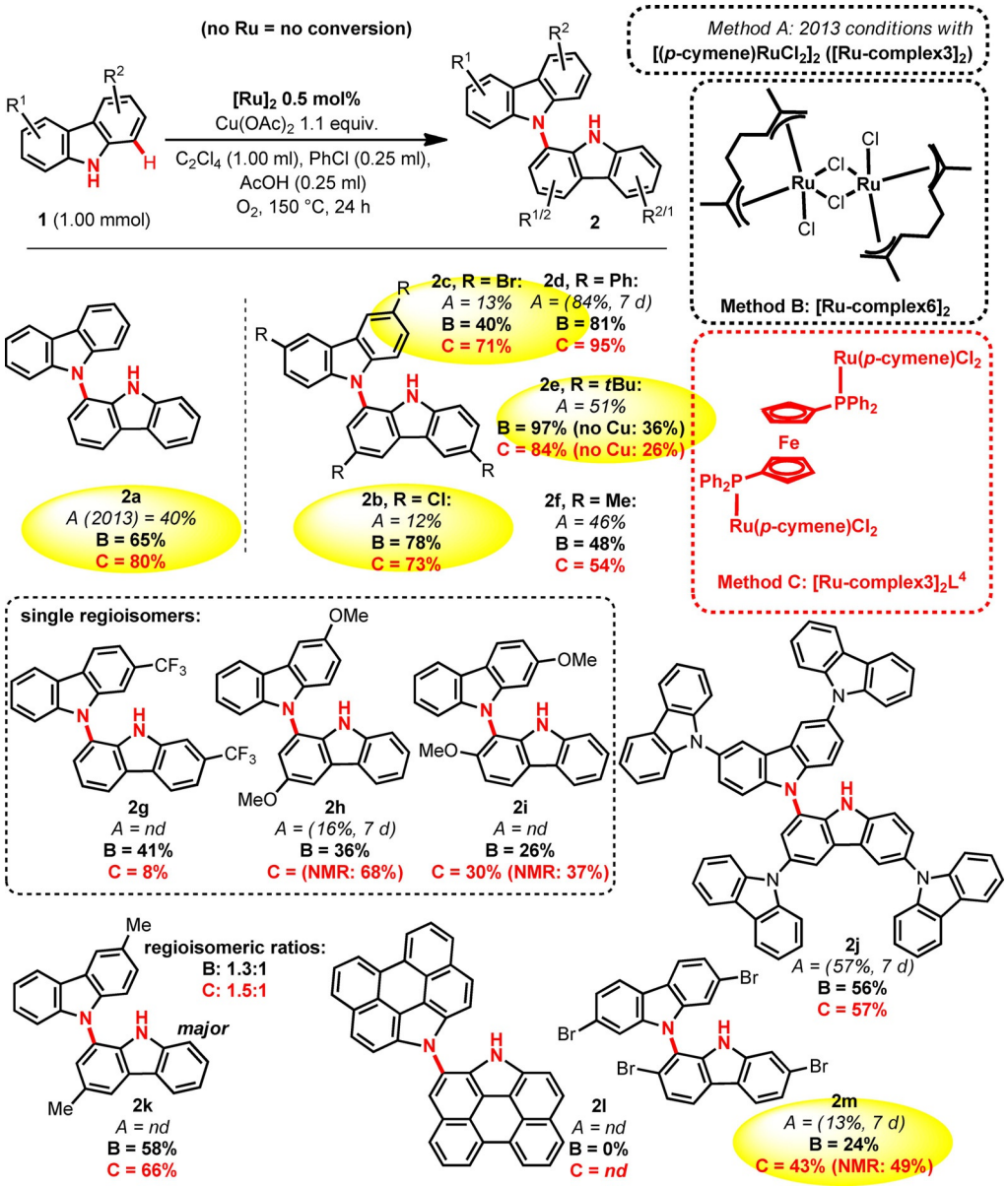

Scheme 1. Comparative reaction scope, isolated yields. A: 2013 reaction conditions: [{Ru(*p*-cymene)Cl_2}$_2$] (0.5 mol%), $Cu(OAc)_2$ (10 mol%), PhCl, C_2Cl_4, AcOH (5:5:1), air, 140 °C. B and C: Carbazole (1.00 mmol), dichlorodi-μ-chlorobis[(1,2,3,6,7,8-η-2,7-dimethyl-2,6-octadiene-1,8-diyl]diruthenium(IV) **[(Ru-complex6)$_2$]** (0.5 mol%) (Method B) or [{Ru(*p*-cymene)Cl_2}$_2$] (0.5 mol%) and 1,1′-bis(diphenylphosphino)ferrocene (0.5 mol%) (**[(Ru-complex3)$_2$L^4]**) (Method C), $Cu(OAc)_2$ (1.1 equiv), C_2Cl_4 (1 mL), PhCl (0.25 mL), AcOH (0.25 mL), O_2, 150 °C, 24 h.

carbazole substrate scope (Scheme 1). Interestingly, not only the yields of existing C1–N bicarbazoles could be improved significantly, but some electron-poor carbazoles were converted for the first time as well. Importantly, no conversion is obtained in the absence of Ru salt. Product **2e** was nevertheless obtained in 36% NMR yield in the absence of the Cu salt while utilizing the **[(Ru-complex6)$_2$]** pre-catalyst, and in only 26% while utilizing the **[(Ru-complex3)$_2$L^4]** pre-catalyst. In these last two cases, however, long reaction times are needed (>1 h) in order to obtain conversion, highlighting the considerable accelerating effect of the Cu salt. Once with these significantly improved sets of reaction conditions in hand, we then performed a series of kinetic experiments in order to probe and characterize their suspected cooperative polynuclear character. These should reveal the precise nature of the cooperative interaction between Ru and Cu in the key steps of the reaction mechanism. For each of the two selected best pre-catalysts (**[(Ru-complex6)$_2$]** and **[(Ru-complex3)$_2$L^4]**), six parallel reactions were first conducted and stopped after 30 min, 1 h, 2 h, 4 h, 6 h, and 24 h, and thereafter analyzed by ^{1}H NMR spectroscopy. Both pre-catalysts clearly allow high initial rates (product **2e**, Figure 1A). Interestingly, for both **[(Ru-complex6)$_2$]** and **[(Ru-complex3)$_2$L^4]**, product formation is very fast in the early stage of the reaction, suggesting the rapid formation of the active species. Further experiments revealed the kinetic orders for Ru, which are surprisingly consistent with an order of +0.4 for both **[(Ru-complex6)$_2$]** and **[(Ru-complex3)$_2$L^4]** (see Supporting Information). This reveals a dependency on Ru for the

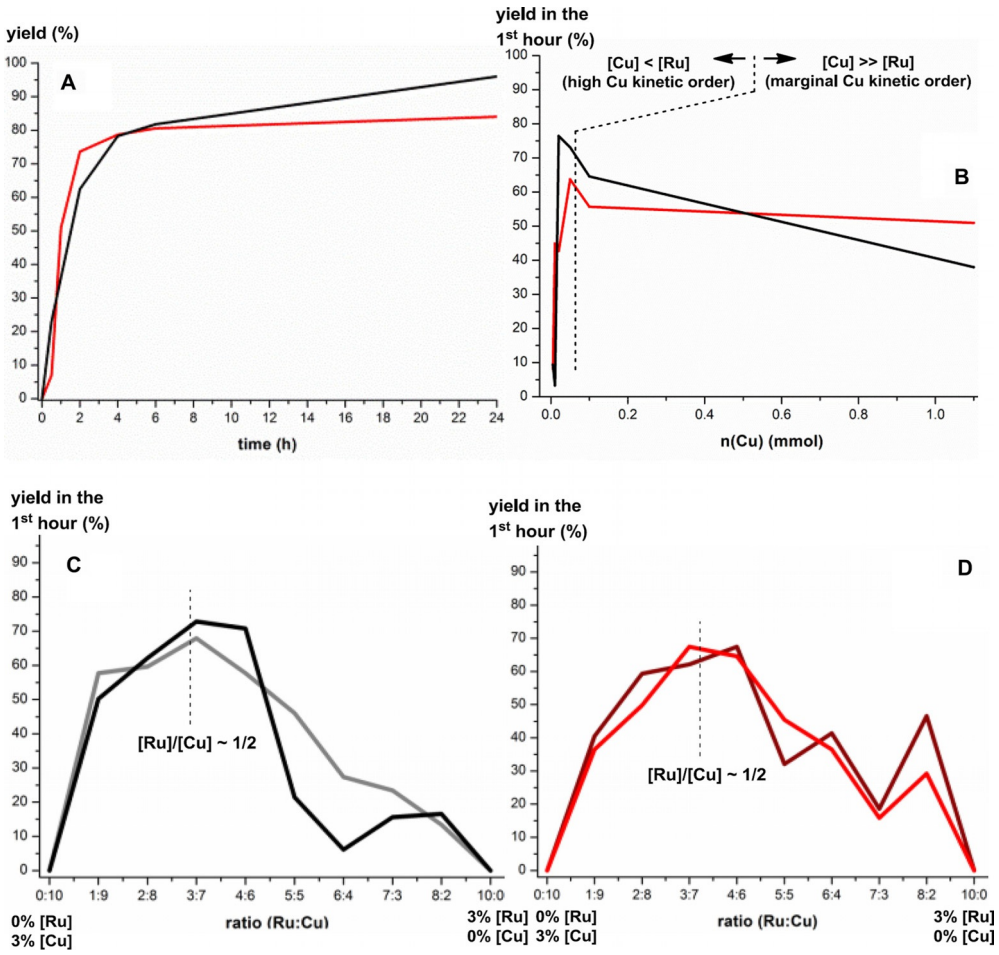

Figure 1. A: ^{1}H NMR conversion to product **2e** over time. B: Dependency of the initial rate ($t = 1$ h) on the Cu loading (mmol). C and D: Initial reactivity Job-plots ($t = 1$ h): [Ru] + [Cu] = 3 mol% for **[(Ru-complex6)$_2$]** and **[(Ru-complex3)$_2$L^4]**, respectively. The second line in respectively C and D represents the reproduced experiments. For all parts black plots for **[(Ru-complex6)$_2$]** and red plots for **[(Ru-complex3)$_2$L^4]**. 1,3,5-Trimethylbenzene was used as an internal standard.

rate-determining step(s). However, the low values (< 1) suggest a dissociation process of the Ru-chloride-bridged homodimers.

Furthermore, at a catalytic loading of 0.125 mol% of Ru, an initial TOF of 144 h^{-1} for **[(Ru-complex6)$_2$]** and an impressive 232 h^{-1} for **[(Ru-complex3)$_2$L^4]** were determined (based on the amount of substrate converted into the product within 1 h). A further decrease of the catalytic loading to 0.0625 mol% improved the initial TOF of **Ru-complex6** to an unprecedented 337 h^{-1}. In 2013, utilizing a far less efficient catalytic system (method A) based on a different temperature, aerobic O_2 partial pressure, solvent ratio, concentration, ligand and carbazole, had afforded an initial TOF of 0.13 h^{-1} (1 mol% of Ru, no reliable conversion detected beneath 0.5 mol% Ru loading).[4a] The initial TOFs of the currently reported systems, in which all the latter parameters were re-optimized, are thus orders of magnitude greater than the previously reported system, and should therefore provide a more precise kinetic picture. We thereafter measured the Cu kinetic orders with both **[(Ru-complex6)$_2$]** and **[(Ru-complex3)$_2$L^4]** systems. In contrast to Ru, the Cu kinetic orders can reach up to +2.5 for the **[(Ru-complex3)$_2$L^4]** system, and up to a surprisingly high +4.7 for the **[(Ru-complex6)$_2$]** system, in the region in which the Cu concentration is small ([Cu] < [Ru], Figure 1B). Importantly, these numbers suggest that multiple Cu association processes would be taking place in the rate-determining step(s) of the reaction. It is quite difficult to assess at this point whether these Cu kinetic orders are exceptional or not, because C–H bond activation studies in which these parameters are measured are rare.[7] Only two computational studies by some of us have previously suggested that the RhCp*/Cu^{II} C–H bond activation system could contain kinetically meaningful polynuclear intermediates.[8]

In the area in which the Cu concentration is large however ([Cu] ≫ [Ru], Figure 1B), the Cu kinetic order breaks down completely to −0.1 for the **[(Ru-complex6)$_2$]** system, and to −0.2 for the **[(Ru-complex3)$_2$L^4]** system. These almost zero orders indicate a saturation point after which the Cu concentration is sufficiently high to spontaneously form the active species. The slightly negative values may even suggest the formation of less active polynuclear aggregates at very high Cu concentrations. This data made us curious as to the actual optimal ratio between Ru and Cu. In order to investigate that particular point, we then conducted what is best described as "reactivity Job-plots",[4a] by analogy with Job-plots experiments that determine the ideal ratio between components of a given supra-

molecular system.[9] The principle here consists in monitoring the initial rate of the reaction, in which the sum of the Ru and the Cu concentration is constant, in this case [Ru]+[Cu]= 3 mol%, but the Ru:Cu ratio is variable, from 0:10 to 10:0. The results for both the **[(Ru-complex6)$_2$]** and **[(Ru-complex3)$_2$L^4]** systems are reported in Figure 1C and D, respectively. The optimal ratio for both systems is reached somewhere around Ru:Cu = 1:2. This shows that a surplus of Cu over Ru is needed to ensure a high catalytic activity and initial TOF, and thereby hints to a trinuclear rate-determining step. Next, H/D scrambling experiments were conducted in order to gain insight into the C–H activation step (Substrate **1a**, see Supporting Information, Figure S3). These were conducted by replacing the acetic acid co-solvent by AcOD, and then monitoring D incorporation. These experiments show a high-to-moderate H/D scrambling under catalytic conditions, depending on reactions conditions, particularly at C1 and C3 positions of the carbazole substrate (C1 > C3). Therefore, the C–H activation step is reversible under catalytic conditions, and thereby probably not rate-limiting. This is an unusual result in the light of the absence of any chelate-assisting directing group. It should be noted that neither conversion, nor any detectable H/D scrambling of **1a** could be observed in the absence of either the copper or the ruthenium salts.

We thereafter looked at the mechanism by using DFT calculations, in consideration of all the above-mentioned kinetic data. Computational details are in the Supporting Information. A data set collection of computational results is available in the ioChem-BD repository[10] and can be accessed via https://doi.org/10.19061/iochem-bd-1-86. For the sake of simplicity, we approximated the catalytic systems to aggregates composed of one Ru center for two Cu centers due to the dimeric character of [Cu(OAc)$_2$] species (the computed dissociation energy for the dimer is 14.7 kcal mol^{-1}). We performed the calculations on the **Ru-complex1** catalyst ([Ru(benzene)Cl$_2$]), as the most simple from a conformational point of view, in the assumption that the general mechanism will be essentially the same for other catalysts. Some of the questions which we were hoping to address with DFT calculations were:

1) Why does this process require both Ru and Cu species, while the oxidative dimerization of other seemingly related substrates such as phenothiazines do not?[11]
2) How are the metal centers interacting in those critical steps and how to characterize their cooperativity?
3) Why is the C1–N the only regio-isomeric product?

We were able to characterize computationally a full catalytic cycle that reproduces all experimental results. It can be separated into four main steps: 1) N–H activation by copper diacetate,[12] 2) Ru-based C–H activation, 3) trinuclear cooperative reductive elimination, and 4) catalyst regeneration. We are going to discuss the first three of these steps in what follows. The reaction starts with the N–H activation by the copper diacetate dimer, shown in Figure 2A. It should be noted that in the drawings we are using a triple-bond between the two copper centers to indicate the presence of three acetate bridges between them. The mechanism, shown in Figure 2A, is formally simple. The most remarkable feature of this step is the spin distribution in the resulting species **3t** and **4t** (see Figure S4 in the Supporting Information). The two unpaired electrons are not fully located on the dicopper system, but one electron is delocalized in the carbazole ring. The process is therefore better described as an oxidative N–H activation, with one electron moving from the nitrogen center to the dicopper unit, which becomes thus Cu^{II}–Cu^{I}.

The next reaction step is the ruthenium-based C–H activation, shown in Figure 2B. Prior to reacting, the ruthenium precatalyst must be activated by molecular oxygen to reach its active form. One dioxygen molecule reacts with two Ru^{II} complexes to produce two complexes **5t**, which can be described as Ru^{III}–oxyl (with radical character on oxygen), or Ru^{IV}–oxo.

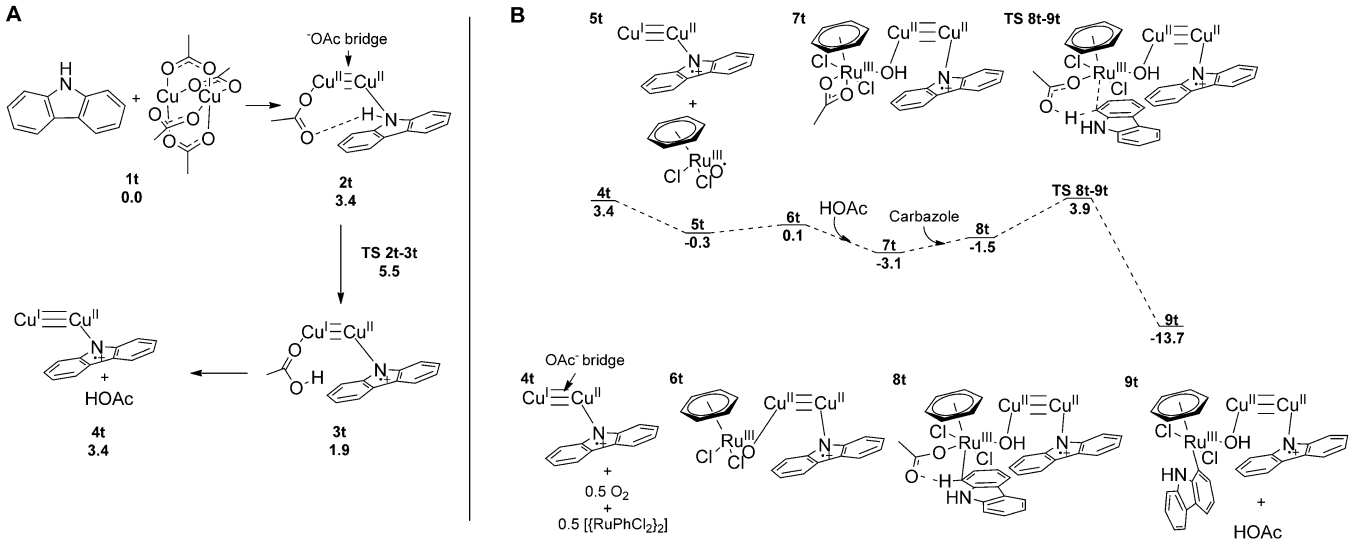

Figure 2. A: Computed pathway for N-H activation of carbazole by copper diacetate dimer. B: Free energy profile for Ru oxidation and C–H bond activation. Energies in kcal mol^{-1}.

The Ru–oxyl moiety has been well characterized in other organometallic ruthenium systems by $^{18}O_2$-labeling mass spectrometry experiments.[13] Intermediate **5t** reacts with the copper complex **4t** to produce the trimetallic complex **7t**. In **7t**, one electron has been transferred from the dicopper unit to the oxyl bridge, which also has been protonated, thus becoming a hydroxo group. As a result, the oxidation states in **7t** are Cu^{II}, Cu^{II}, and Ru^{III}, with additional free radical character in the carbazole. Intermediate **7t** is then able to activate the C–H bond of a second carbazole unit through a CMD (concerted metalation deprotonation) mechanism.[14] From an electron-count point of view, this complex step from **4t** to **9t** results in the acquisition of two electrons per oxygen atom of the initial molecular dioxygen reagent, one coming from ruthenium and another from the dicopper unit. An alternative pathway for C–H activation without formation of the trimetallic species was found to have a much higher barrier (see Supporting Information).

The next step is reductive elimination, shown in Figure 3. The system evolves through a trinuclear cooperative reductive elimination (CRE) transition state to form the C–N bond. This is related to the process some of us characterized for the oxidative coupling of benzoic acid and alkyne.[8,15] The free-energy barrier of this process is 24.2 kcal mol^{-1}, with respect to the most stable intermediate **9t**. The structure of transition state **TS 10t–11t** is presented in Figure 3. The electron count from this step is quite simple: a single electron transfer from the formally anionic carbon ligand to ruthenium, which becomes Ru^{II}. This is very different from what we found for the Rh^{III}/Cu^{II} system,[8] in which one electron was transferred to each metal center. The common feature is the requirement of three metal centers, and the relevance of single electron transfer processes throughout the catalytic cycle. Importantly, this reductive elimination step is irreversible and it is the rate-determining step for the **Ru-complex1** catalyst. Modifications in other ligands could change the rate-determining step to C–H cleavage through **TS 8t–9t**, which is 6.6 kcal mol^{-1} below **TS 10t–11t** for the **Ru-complex1**. The finding that the key transition states contain two copper and one ruthenium centers is an encouraging agreement with the experimentally determined orders of reactions. We remark that we did not consider further aggregations of copper centers for simplicity, but they could well exist and push further the reaction order with respect to copper. Finally, the initial catalysts are regenerated, releasing water as a byproduct, with an overall energy release of 35.6 kcal mol^{-1}. This regeneration step, detailed in the Supporting Information, does not involve major electron flows, as the three metal centers have already recovered their initial oxidation states.

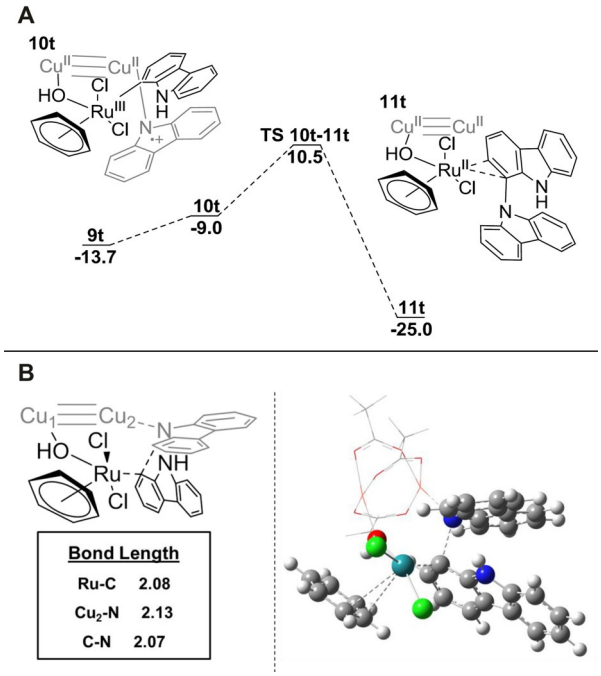

Figure 3. Computational results on the cooperative reductive elimination step. A: Free energy profile. Energies in kcal mol^{-1}. B: **TS 10t–11t** in 2D view. Representative bond distances in Å. **TS 10t–11t** in 3D view. The copper dimer is depicted in wireframe for clarity.

After characterizing the full mechanism, we analyzed the issue of selectivity. We need to reproduce two sets of experimental results from the **Ru-complex3** catalyst ([Ru(*p*-cymene)Cl_2]), which is very similar to the **Ru-complex1** system considered for the calculations. Deuterium scrambling experiments show that the C–H bond can be activated at three different positions in the activity order of C1 > C3 > C2 (see Supporting Information Figure S3), yet the formation of a bond with nitrogen occurs only at C1. The irreversible step in our calculations is the cooperative reductive elimination through **TS 10t–11t**. The energy of this transition state with respect to separate reactants is 10.5 kcal mol^{-1} for C1, as discussed above. We calculated the corresponding values for C2 and C3 cooperative reductive eliminations and both are higher than **TS 10t–11t** (16.9 and 14.2 kcal mol^{-1} above the reactants, respectively). The difference between C1 and C3 transition state is 3.7 kcal mol^{-1}, which corresponds to a theoretical prediction of > 99% of the homo-coupling product at C1. In contrast, C–H activation has a lower barrier, and scrambling can take place prior to the irreversible step. The values associated with the transition states associated to the activation of the different positions were 3.9 (C1), 8.5 (C2), 4.5 (C3), and 10.6 (C4) kcal mol^{-1} with respect to the reactants. Bonds to C1, C2 and C3 can be activated, which is in agreement with experimental data.

In summary, we identified two new Ru-based C–H bond activation systems based on pre-catalysts **[(Ru-complex6)$_2$]** and **[(Ru-complex3)$_2$L^4]**, which are orders of magnitude more active in the herein studied C–H bond activation coupling reaction. Moreover, kinetic studies revealed the probable involvement of cooperative polymetallic Ru/Cu (1:2) aggregates in the rate-determining step. The latter cooperative reductive elimination (CRE) step demonstrates that the electronic connection between metals is necessary for an efficient process. The computed CRE transition state moreover rationalized the exclusive C1 selectivity of the reaction, versus C2 and C3, as these last positions show significantly higher reductive elimination transition states. Because of their pronounced polynuclear cooperative character, these results might impact the field of CDC

method development, particularly those methods that are based on bimetallic Ru/Cu, Rh/Cu and Pd/Cu catalyzed C–H bond activation systems.

Acknowledgements

This work was supported by DFG-funded transregional collaborative research center SFB/TRR 88 "Cooperative effects in homo and heterometallic complexes" (http://3MET.de), DFG funded project PA 2395/2-1, COST Action CA15106 (CHAOS), and since March 2017: by ERC project 716136: "2O2ACTIVATION". F.M. acknowledges the financial support from the CERCA Programme/Generalitat de Catalunya and MINECO (Project CTQ2017-87792-R and Severo Ochoa Excellence Accreditation 2014–2018 (SEV-2013-0319)) and I.F.-A thanks the Severo Ochoa predoctoral training fellowship (ref: SVP-2014–068662). We thank Dr. Agostino Biafora for fruitful discussions. Tristan Weiser and Ann-Katrin Seitz are acknowledged for short internships in the Patureau group. Tatjana Wall is acknowledged for the microbalance equipment.

Conflict of interest

The authors declare no conflict of interest.

Keywords: C–H bond activation · cooperative reductive elimination · cross dehydrogenative coupling · dehydrogenative amination · trinuclear catalysis

[1] Polynuclear catalysis, see for example: a) R. G. Bergman, *Acc. Chem. Res.* **1980**, *13*, 113; b) T. Fukuyama, N. Chatani, J. Tatsumi, F. Kakiuchi, S. Murai, *J. Am. Chem. Soc.* **1998**, *120*, 11522; c) J. Kwak, M. Kim, S. Chang, *J. Am. Chem. Soc.* **2011**, *133*, 3780; d) M. M. Lorion, K. Maindan, A. R. Kapdi, L. Ackermann, *Chem. Soc. Rev.* **2017**, *46*, 7399.

[2] C –H bond functionalization: see for example: a) C.-L. Sun, B.-J. Li, Z.-J. Shi, *Chem. Commun.* **2010**, *46*, 677; b) C. S. Yeung, V. M. Dong, *Chem. Rev.* **2011**, *111*, 1215; c) L. McMurray, F. O'Hara, M. J. Gaunt, *Chem. Soc. Rev.* **2011**, *40*, 1885; d) P. B. Arockiam, C. Bruneau, P. H. Dixneuf, *Chem. Rev.* **2012**, *112*, 5879; e) J. Yamaguchi, A. D. Yamaguchi, K. Itami, *Angew. Chem. Int. Ed.* **2012**, *51*, 8960; *Angew. Chem.* **2012**, *124*, 9092; f) S. I. Kozhushkov, L. Ackermann, *Chem. Sci.* **2013**, *4*, 886; g) C. Liu, J. Yuan, M. Gao, S. Tang, W. Li, R. Shi, A. Lei, *Chem. Rev.* **2015**, *115*, 12138; h) T. Gensch, M. N. Hopkinson, F. Glorius, J. Wencel-Delord, *Chem. Soc. Rev.* **2016**, *45*, 2900; i) Y. Qin, L. Zhu, S. Luo, *Chem. Rev.* **2017**, *117*, 9433; j) D.-S. Kim, W.-J. Park, C.-H. Jun, *Chem. Rev.* **2017**, *117*, 8977.

[3] Amination methods, see for example: a) F. Ullmann, *Ber. Dtsch. Chem. Ges.* **1903**, *36*, 2382; b) I. Goldberg, *Ber. Dtsch. Chem. Ges.* **1906**, *39*, 1691; c) J. F. Hartwig, *Nature* **2008**, *455*, 314; d) J. F. Hartwig, *Acc. Chem. Res.* **2008**, *41*, 1534; e) D. S. Surry, S. L. Buchwald, *Angew. Chem. Int. Ed.* **2008**, *47*, 6338; *Angew. Chem.* **2008**, *120*, 6438; f) J. Bariwal, E. van der Eycken, *Chem. Soc. Rev.* **2013**, *42*, 9283; g) M.-L. Louillat, F. W. Patureau, *Chem. Soc. Rev.* **2014**, *43*, 901; h) P. Ruiz-Castillo, S. L. Buchwald, *Chem. Rev.* **2016**, *116*, 12564; i) Z. Li, H. Yu, C. Bolm, *Angew. Chem. Int. Ed.* **2017**, *56*, 9532; *Angew. Chem.* **2017**, *129*, 9660; j) Y. Park, Y. Kim, S. Chang, *Chem. Rev.* **2017**, *117*, 9247; k) J. Schranck, A. Tlili, *ACS Catal.* **2018**, *8*, 405.

[4] Selected examples: a) M.-L. Louillat, F. W. Patureau, *Org. Lett.* **2013**, *15*, 164; b) M.-L. Louillat, A. Biafora, F. Legros, F. W. Patureau, *Angew. Chem. Int. Ed.* **2014**, *53*, 3505; *Angew. Chem.* **2014**, *126*, 3573; c) A. Biafora, F. W. Patureau, *Synlett* **2014**, *25*, 2525; d) J. Roane, O. Daugulis, *J. Am. Chem. Soc.* **2016**, *138*, 4601; e) J. Jiao, K. Murakami, K. Itami, *ACS Catal.* **2016**, *6*, 610.

[5] Natural product containing the C1-N bicarbazole: Z. Xu, M. Baunach, L. Ding, C. Hertweck, *Angew. Chem. Int. Ed.* **2012**, *51*, 10293; *Angew. Chem.* **2012**, *124*, 10439.

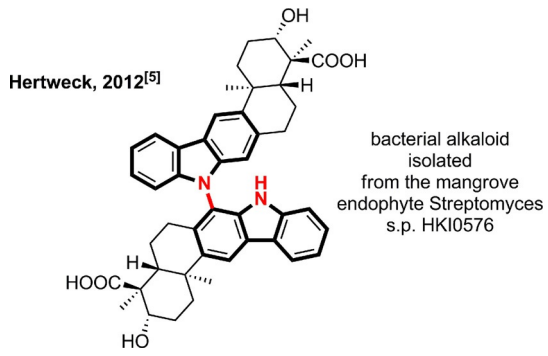

[6] L. Ackermann, S. I. Kozhushkov, D. S. Yufit, *Chem. Eur. J.* **2012**, *18*, 12068.

[7] Nevertheless, the well-documented propensity of copper-O_2 systems to form oxo-bridged polynuclear intermediates suggests that high copper kinetic orders should be ubiquitous in copper-catalyzed aerobic transformations. See for example: a) M. El-Sayed, A. El-Toukhy, G. Davies, *Inorg. Chem.* **1985**, *24*, 3387; b) P. Haack, C. Limberg, *Angew. Chem. Int. Ed.* **2014**, *53*, 4282; *Angew. Chem.* **2014**, *126*, 4368, and references therein.

[8] a) I. Funes-Ardoiz, F. Maseras, *Angew. Chem. Int. Ed.* **2016**, *55*, 2764; *Angew. Chem.* **2016**, *128*, 2814; b) I. Funes-Ardoiz, F. Maseras, *Chem. Eur. J.* **2018**, *24*, 12383.

[9] J. S. Renny, L. L. Tomasevich, E. H. Tallmadge, D. B. Collum, *Angew. Chem. Int. Ed.* **2013**, *52*, 11998; *Angew. Chem.* **2013**, *125*, 12218.

[10] M. Álvarez-Moreno, C. de Graaf, N. Lopez, F. Maseras, J. M. Poblet, C. Bo, *J. Chem. Inf. Model.* **2015**, *55*, 95.

[11] Several N–H heterocyclic substrates, including particularly electron-rich carbazoles, have been known to oxidize without precious-metal-catalyzed C–H bond activation, sometimes in the mere presence of a mild oxidant. However, so far, the C1–N bicarbazole coupling products depicted in Scheme 1 can only be obtained with the herein described Ru–Cu co-catalyzed method. The fact that the omission of the Ru salt completely suppresses conversion arguably suggests that a free-radical mechanism is unlikely. For those other more electron-rich, easily oxidized N–H heterocyclic substrates, such as phenothiazines, see for example: a) M. Goswami, A. Konkel, M. Rahimi, M.-L. Louillat-Habermeyer, H. Kelm, R. Jin, B. de Bruin, F. W. Patureau, *Chem. Eur. J.* **2018**, *24*, 11936; b) M.-L. Louillat-Habermeyer, R. Jin, F. W. Patureau, *Angew. Chem. Int. Ed.* **2015**, *54*, 4102; *Angew. Chem.* **2015**, *127*, 4175; c) C. Schuster, C. Börger, K. K. Julich-Gruner, R. Hesse, A. Jäger, G. Kaufmann, A. W. Schmidt, H.-J. Knölker, *Eur. J. Org. Chem.* **2014**, 4741; d) J. A. van Allan, G. A. Reynolds, D. P. Maier, *J. Org. Chem.* **1969**, *34*, 1691; e) R. F. Bridger, D. A. Law, D. F. Bowman, B. S. Middleton, K. U. Ingold, *J. Org. Chem.* **1968**, *33*, 4329; f) Y. Tsujino, *Tetrahedron Lett.* **1968**, *9*, 4111; g) H. Musso, *Chem. Ber.* **1959**, *92*, 2873; h) H. Wieland, A. Süßer, *Justus Liebigs Ann. Chem.* **1912**, *392*, 169; i) palladium-catalyzed examples: R. Gu, K. Van Hecke, L. Van Meervelt, S. Toppet, W. Dehaen, *Org. Biomol. Chem.* **2006**, *4*, 3785; j) B. Liégault, D. Lee, M. P. Huestis, D. R. Stuart, K. Fagnou, *J. Org. Chem.* **2008**, *73*, 5022.

[12] Selected examples of $Cu(OAc)_2$-mediated oxidative N–H activation/functionalization: a) G. Brasche, S. L. Buchwald, *Angew. Chem. Int. Ed.* **2008**, *47*, 1932; *Angew. Chem.* **2008**, *120*, 1958; b) D. Monguchi, T. Fujiwara, H. Furukawa, A. Mori, *Org. Lett.* **2009**, *11*, 1607; c) H. Zhao, M. Wang, W. Su, M. Hong, *Adv. Synth. Catal.* **2010**, *352*, 1301; d) A. John, K. M. Nicholas, *J. Org. Chem.* **2011**, *76*, 4158; e) M. Miyasaka, K. Hirano, T. Satoh, R. Kowalczyk, C. Bolm, M. Miura, *Org. Lett.* **2011**, *13*, 359; f) L. D. Tran, J. Roane, O. Daugulis, *Angew. Chem. Int. Ed.* **2013**, *52*, 6043; *Angew. Chem.* **2013**, *125*, 6159; g) H. Xu, X. Qiao, S. Yang, Z. Shen, *J. Org. Chem.* **2014**, *79*, 4414; h) B. K. Singh, A. Polley, R. Jana, *J. Org.*

Chem. **2016**, *81*, 4295; i) P. Sadhu, T. Punniyamurthy, *Chem. Commun.* **2016**, *52*, 2803.
[13] R. Ray, S. Chandra, D. Maiti, K. L. Lahiri, *Chem. Eur. J.* **2016**, *22*, 8814.
[14] I. Özdemir, S. Demir, B. Cetinkaya, C. Gourlaouen, F. Maseras, C. Bruneau, P. H. Dixneuf, *J. Am. Chem. Soc.* **2008**, *130*, 1156.
[15] I. Funes-Ardoiz, F. Maseras, *ACS Catal.* **2018**, *8*, 1161.

Manuscript received: June 5, 2018
Accepted manuscript online: June 21, 2018
Version of record online: September 11, 2018

